Supplementary Information

Ultralow detection limit and high sensitivity X-ray detector of high-quality $MAPbBr_3$ perovskite single crystals

Dong Liu[a], Xue Sun[b], Li Jiang[a], Xianyuan Jiang[c], Hao Chen[d], Fucai Cui[b], Guodong Zhang*[b], Yong Wang[a], Ying-Bo Lu[a], Zhongchen Wu*[a], Zhijun Ning[c], and Xutang Tao[b]

[a] School of Space Science and Physics, Institute of Space Sciences, Shandong University, Weihai 264209, China.

[b] State Key Laboratory of Crystal Materials, Institute of Crystal Materials, Shandong University, Jinan 250100, China.

[c] School of Physical Science and Technology, ShanghaiTech University, Shanghai 201210, China.

[d] The Edward S. Rogers Department of Electrical and Computer Engineering, University of Toronto, Toronto, Ontario M5S 3G4, Canada.

† Electronic Supplementary Information (ESI) available.

* **Corresponding authors:** z.c.wu@sdu.edu.cn; zgd@sdu.edu.cn.

Equation S1

The dark current drift, which is used to evaluate the degree of dark current drift, is expressed as:

$$Drift = \frac{J_t - J_0}{t \cdot E}$$

where J_t and J_0 are the current densities at the beginning and end points, respectively; E is the electric field; and t is the duration.

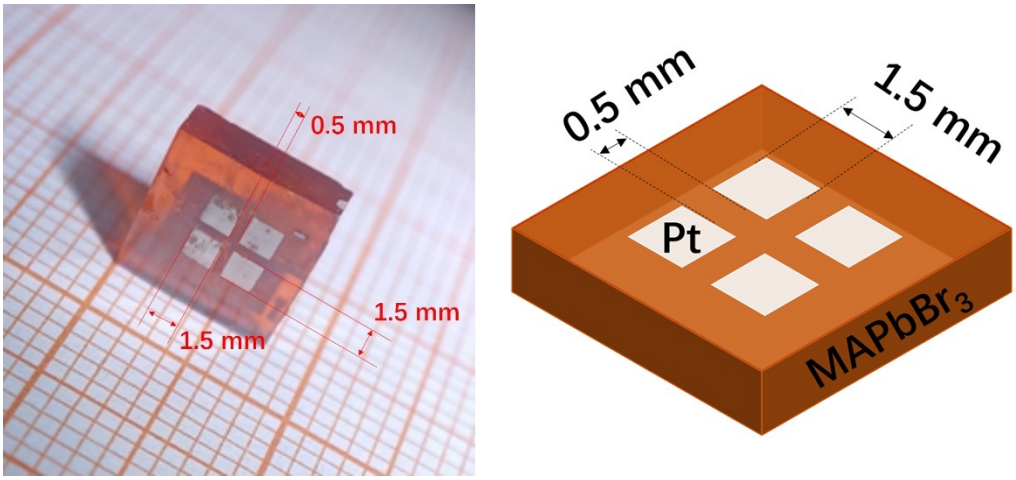

Fig. S1. Photograph of the VEC-$MAPbBr_3$ single crystal device structure.

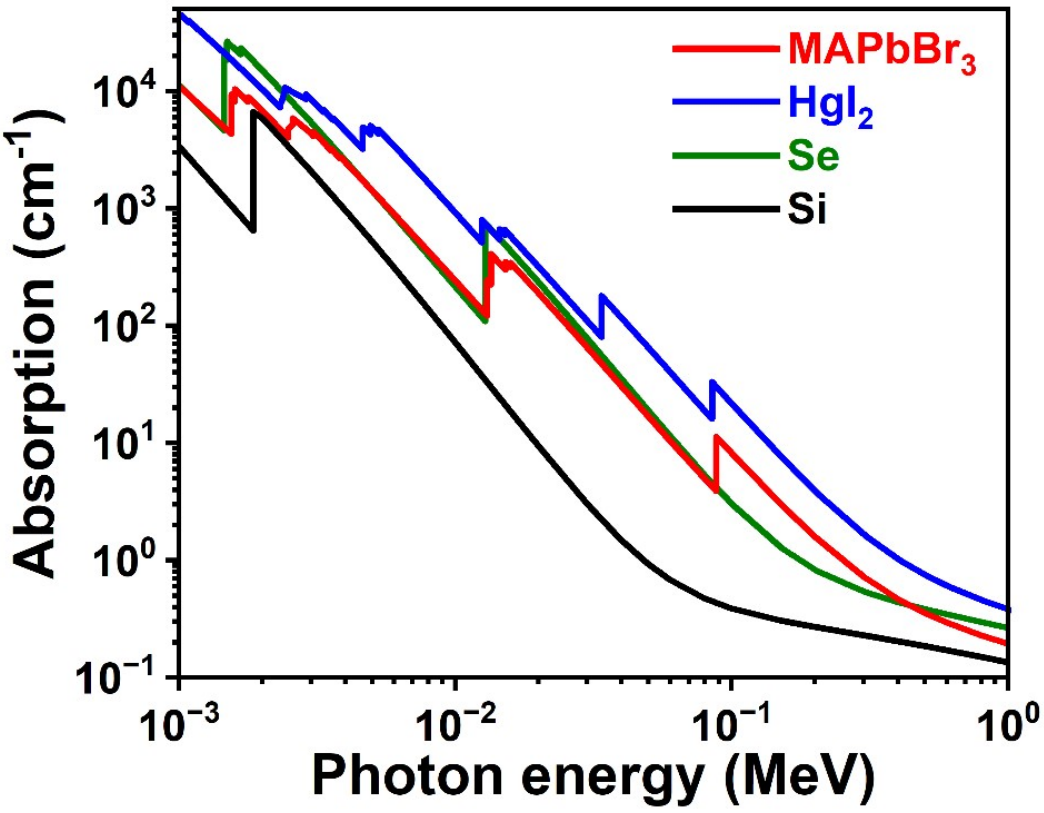

Fig. S2. Linear absorption coefficients of $MAPbBr_3$, HgI_2, Se, and Si as a function of photo energy from 0.001 to 1 MeV.

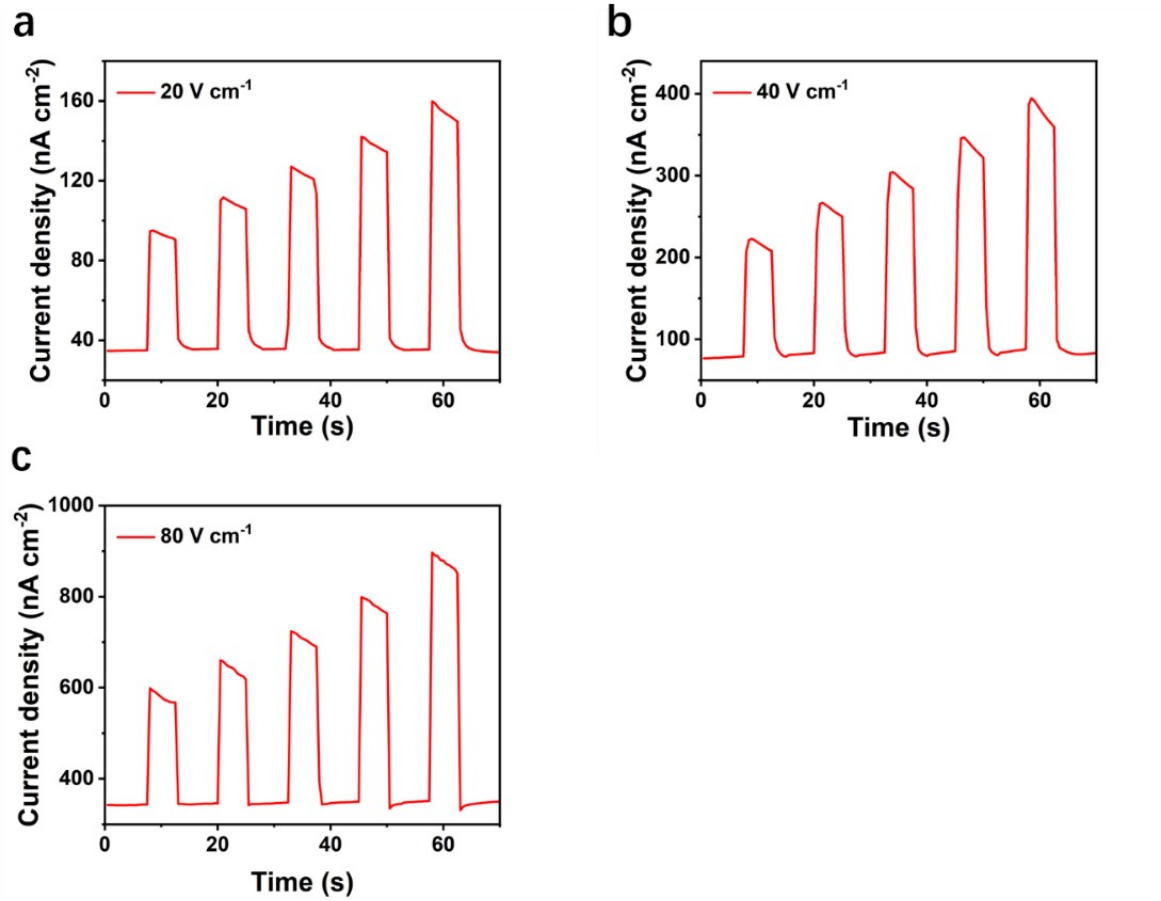

Fig. S3. Photocurrent-dose rate curves of the LPAC-$MAPbBr_3$ detector at electric fields strengths of 20, 40, and 80 V cm^{-1}.

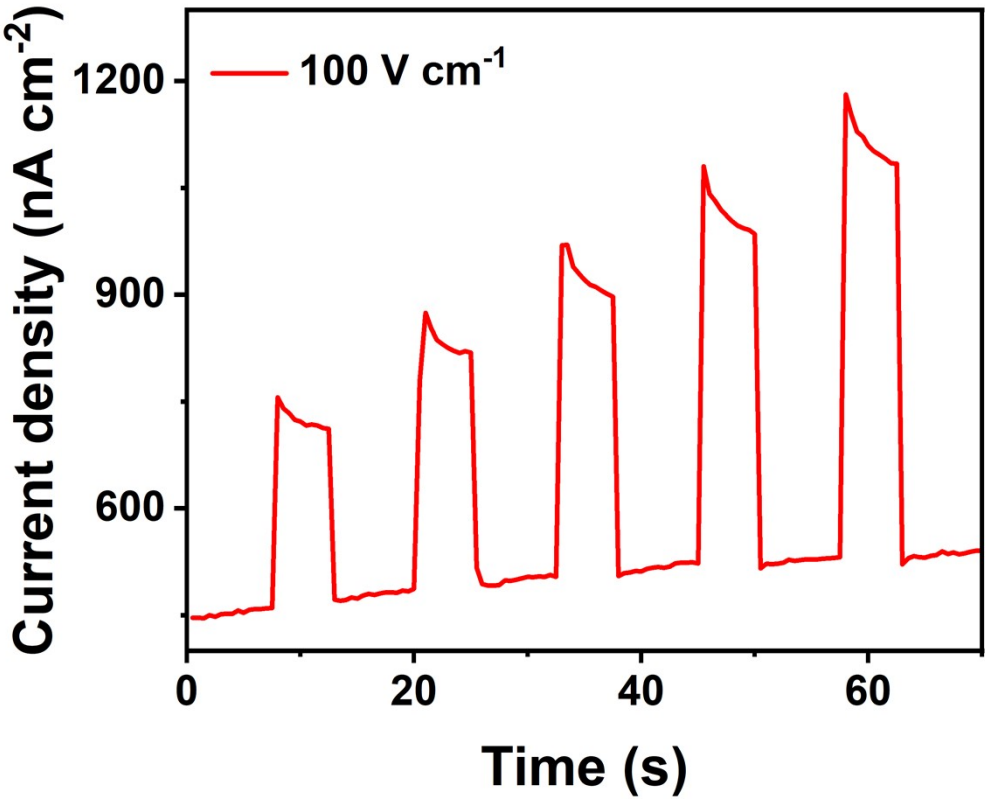

Fig. S4. Photocurrent-dose rate curves of the detector at an electric field strength of 100 V cm^{-1}.

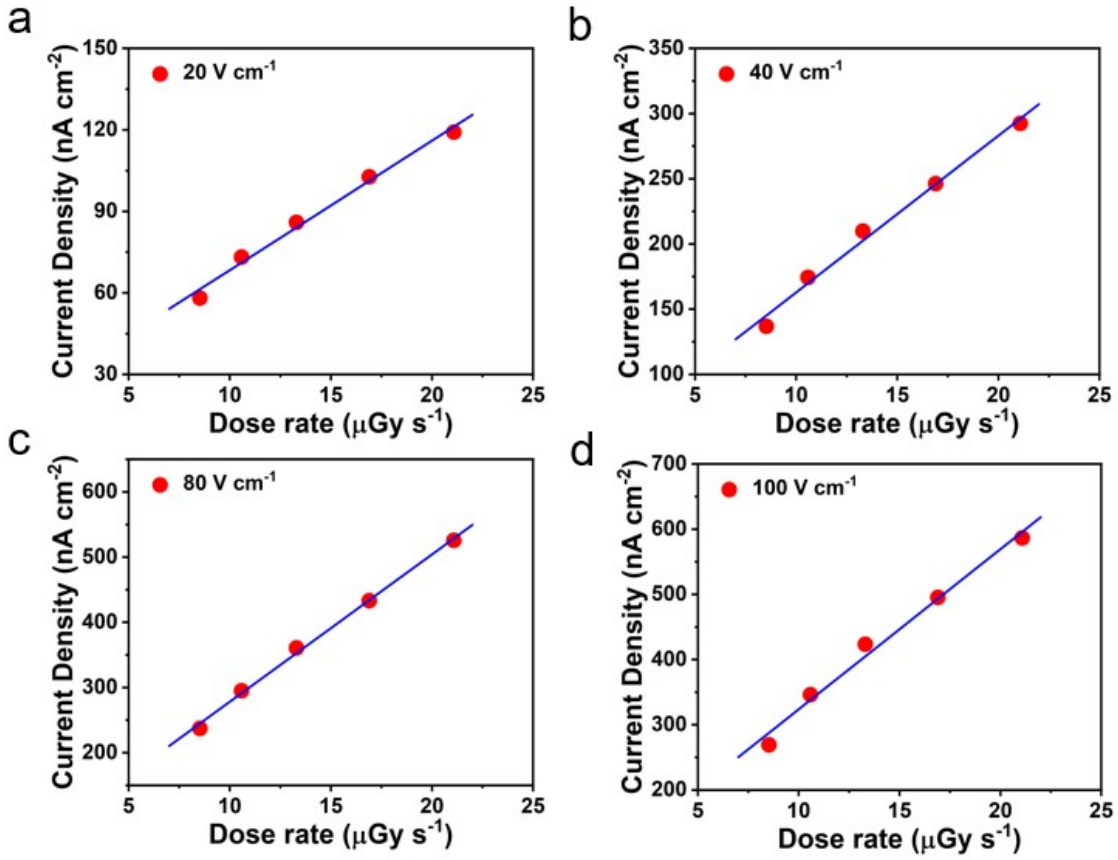

Fig. S5. Photocurrent response of the detector at different electric field strengths and various dose rates under 100 kV_p X-ray illumination.

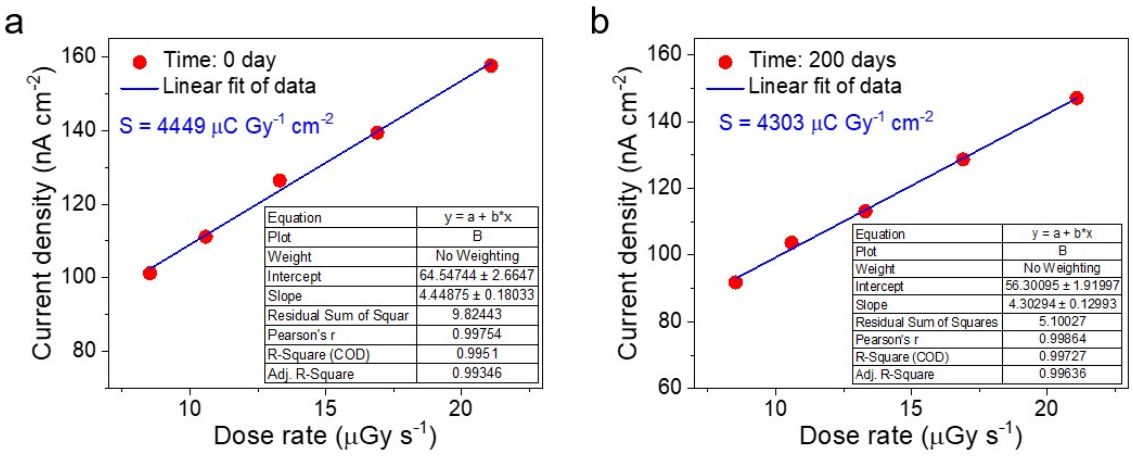

Fig. S6. Photocurrent response of the detector was assessed under 100 kV_p X-ray illumination at various dose rates, and the sensitivities were evaluated on day 0 and day 200.

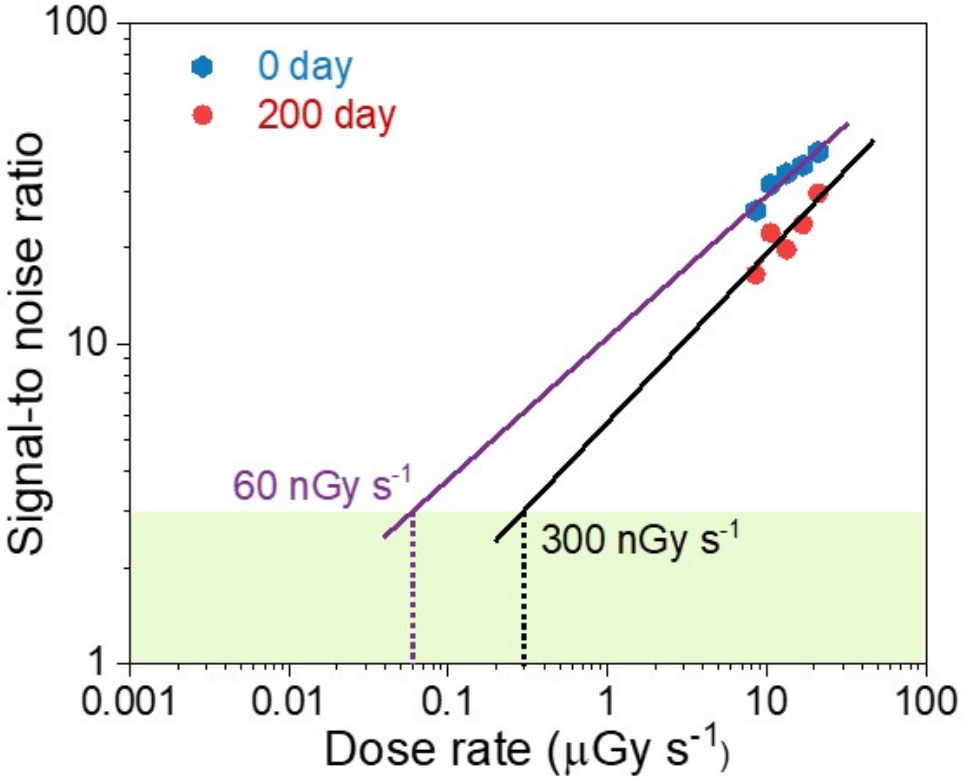

Fig. S7. Signal-to-noise ratio of the VEC-$MAPbBr_3$ SC detector on day 0 and day 200.

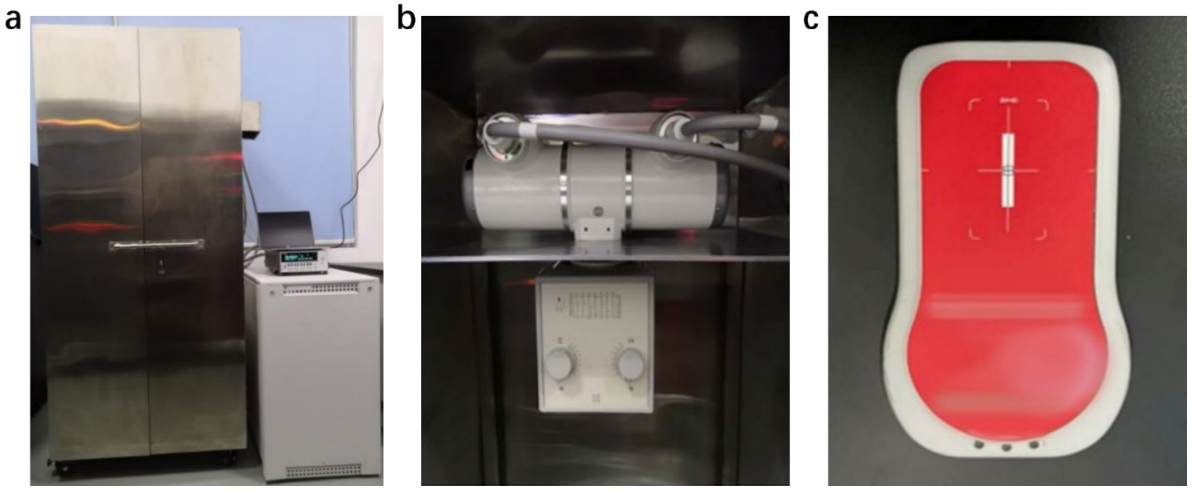

Fig. S8. Photographs of (a) the X-ray-generating and shielding device, (b) the X-ray tube and beam limiter, and (c) the Piranha 655 X-ray machine multifunctional quality detector.

Table S1. Summary of detailed fitting parameters of time-resolved photoluminescence (TRPL) spectroscopy for VEC-$MAPbBr_3$ and HT- $MAPbBr_3$.

Sample	VEC-$MAPbBr_3$	HT- $MAPbBr_3$
Model	ExpDec2	
Equation	$y = A_1 e^{-\frac{x}{\tau_1}} + A_2 e^{-\frac{x}{\tau_2}} + y_0$	
y_0	8.5657 ± 1.77196	4.94962 ± 0.85886
A_1	2006.22578 ± 13.05686	1947.27637 ± 17.06467
τ_1	154.4088 ± 1.86672	143.61114 ± 1.75293
A_2	330.27302 ± 11.48534	377.08082 ± 17.51037
τ_2	1149.76857 ± 49.00642	683.35276 ± 24.72292

Table S2. The detailed fitting results of the *I-V* curve for VEC-$MAPbBr_3$ single crystal.

VEC-$MAPbBr_3$ single crystal			
Regimes	n = 1	n > 3	n = 2
Equation	y = a + b*x	y = a + b*x	y = a + b*x
Intercept	-8.75046 ± 0.01478	-11.3941 ± 0.09745	-8.2387 ± 0.01255
Slope	0.62977 ± 0.03057	3.76295 ± 0.07651	1.56053 ± 0.00687
Residual Sum of Squares	8.54E-04	0.06082	0.00264
Pearson's r	0.99649	0.99589	0.99941
R-Square (COD)	0.99298	0.9918	0.99882
Adj. R-Square	0.99064	0.99139	0.9988

Table S3. The detailed fitting results of the *I-V* curve for HT-$MAPbBr_3$ single crystal.

HT-$MAPbBr_3$ single crystal			
Regimes	n = 1	n > 3	n = 2
Equation	y = a + b*x	y = a + b*x	y = a + b*x
Intercept	-8.00305 ± 0.00875	-9.47216 ± 0.0285	-8.38832 ± 0.03839
Slope	0.92236 ± 0.0111	2.13839 ± 0.01935	1.51949 ± 0.02021
Residual Sum of Squares	0.00146	0.00401	0.00278
Pearson's r	0.99928	0.99894	0.99657
R-Square (COD)	0.99855	0.99788	0.99315
Adj. R-Square	0.99841	0.99779	0.99297

Table S4. Summary of $MAPbBr_3$ SC properties and photodetector performances of resulting X-ray detectors in published representative work.

Ref.	Methods	FWHM of rocking curve (°)	Eg (eV)	PL peak (nm)	τ (ns)	n_{trap} ($\times 10^9$ cm^{-3})	Mobility μ ($cm^2V^{-1}s^{-1}$)	Lowest detectable dose rate ($\mu Gy \cdot S^{-1}$)	Sensitivity ($\mu C\ Gy^{-1}cm^{-2}$)
[1]	LDSC.1	0.0096 (200)	2.15	577	997	4.4		1.2	184.6
[2]	LDSC.2	0.0096 (100)	2.18	577	1099	4.5	88.6		2181
[3]	LTGC.1	0.013 (200)	2.24	545	962	5.2	81		
[4]	LTGC.2	0.019 (100)	2.24	547	897	6.7	83.9		
[5]	PA-ITC.1	0.008 (200)		533	44.87			0.087	15280
[6]	PA-ITC.2	0.127 (100)	2.23	546	923	6.6	39		
[7]	SL-ITC		2.16		17.14	16.9	60		632
[8]	RT-ITC	0.0253	2.29			6.59	18		
	ZT-ITC	0.0179				3.06	6		
	LT-ITC	0.0171				2.55	115		
[9]	AVC.1		2.21	570	978	5.8	115		
[10]	AVC.2			550			217	0.5	80
[11]	AVC.3		2.21				59.7		
[12]	AVC.4			542	242.8	7.96	35		
[13]	VTC		2.19			5.64	27.5	0.35	307
[14]	CGC	0.018 (110)	2.25						
[15]	STCAD	0.0112 (110)	2.3		411.47				426.43
[16]	LCMC	0.0123 (200)	2.17	578	1126	2.1	87.8	0.48	2975.7
[17]	ITC.1		2.18	574	300	30	24		
[18]	ITC.2			550	981	60	2.7		
[19]	ITC.3		2.24	537		26	4.36		
[20]	ITC.4				692		201	0.1	21000
[21]	PTG	0.00806 (100)	2.2	562	1002	4.25		0.67	7275
	VEC	0.00922 (001)	2.20	579	1150	2.28	130	0.054	24552

Table S5. Dose rate calibration for 100 kVp X-ray illumination.

Tube current (mA)	Dose rate 1 (μGy s^{-1})	Dose rate 2 (μGy s^{-1})	Dose rate 3 (μGy s^{-1})	Average dose rate (μGy s^{-1})
10	8.504	8.541	8.532	8.525666667
12.5	10.5	10.67	10.58	10.58333333
16	13.28	13.45	13.18	13.30333333
20	16.79	17.1	16.8	16.89666667
25	20.9	21.54	20.82	21.08666667

References

1 F. Yao, J. Peng, R. Li, P. Li, B. Li, C. Liu, C. Tao, Q. Lin and G Fang, *Nat. Commun.*, 2020, **11**, 1194.

2 Z. Zhang, H. Li, H. Di, D. Liu, W. Jiang, J. Ren, Z. Fan, F. Liao, L. Lei, G. Li, Y. Xiong and Y. Zhao, *ACS Appl. Electron. Mater.*, 2023, **5**, 388-396.

3 Y. Liu, Y. Zhang, K. Zhao, Z. Yang, J. Feng, X. Zhang, K. Wang, L. Meng, H. Ye, M. Liu and S. F. Liu, *Adv. Mater.*, 2018, **30**, 1707314.

4 Y. Liu, Y. Zhang, Z. Yang, J. Feng, Z. Xu, Q. Li, M. Hu, H. Ye, X. Zhang, M. Liu, K. Zhao and S. F. Liu, *Mater. Today*, 2019, **22**, 67-75.

5 L. Chen, H. Wang, W. Zhang, F. Li, Z. Wang, X. Wang, Y. Shao and J. Shao, *ACS Appl. Mater. Interfaces*, 2022, **14**, 10917-10926.

6 L. Ma, Z. Yan, X. Zhou, Y. Pi, Y. Du, J. Huang, K. Wang, K. Wu, C. Zhuang and X. Han, *Nat. Commun.*, 2021, **12**, 2023.

7 A. Feng, S. Xie, X. Fu, Z. Chen and W. Zhu, *Front. Chem.* 2022, **9**, 823868.

8 Y. Cho, H. R. Jung, Y. S. Kim, Y. Kim, J. Park, S. Yoon, Y. Lee, M. Cheon, S.-Y. Jeong and W. Jo, *Nanoscale* 2021, **13**, 8275-8282.

9 D. Shi, V. Adinolfi, R. Comin, M. Yuan, E. Alarousu, A. Buin, Y. Chen, S. Hoogland, A. Rothenberger, K. Katsiev, Y. Losovyj, X. Zhang, P. A. Dowben, O. F. Mohammed, E. H. Sargent and O. M. Bakr, *Science*, 2015, **347**, 519-522.

10 H. Wei, Y. Fang, P. Mulligan, W. Chuirazzi, H.-H. Fang, C. Wang, B. R. Ecker, Y. Gao, M. A. Loi, L. Cao and J. Huang, *Nat. Photonics*, 2016, **10**, 333-339.

11 X. Liu, H. Zhang, B. Zhang, J. Dong, W. Jie and Y. Xu, *J. Phys. Chem. C* 2018, **122**, 14355-14361.

12 S. Rong, Y. Xiao, J. Jiang, Q. Zeng and Y. Li, *J. Phys. Chem. C* 2020, **124**, 8992-8998.

13 X. Wang, D. Zhao, Y. Qiu, Y. Huang, Y. Wu, G. Li, Q. Huang, Q. Khan, A. Nathan, W. Lei and J. Chen, *Phys. Status Solidi RRL* 2018, **12**,1800380.

14 N. I. Selivanov, A. O. Murzin, V. I. Yudin, Y. V. Kapitonov and A. V. Emeline, *CryEngComm* 2022, **24**, 2976-2981.

15 L. Zhang, S. Cui, Q. Guo, C. Ge, Q. Han, Q. Lin, C. Li, X. Zheng, Z. Zhai, L. Wang, Q. Sun, Y. Xu, Y. Liu and X. Tao, *ACS Appl. Mater. Interfaces* 2020, **12**, 51616-51627.

16 Z. Zhu, W. Li, W. Deng, W. He, C. Yan, X. Peng, X. Zeng, Y. Gao, X. Fu, N. Lin, B. Gao and W. Yang,

J. Mater. Chem. C 2022, **10**, 6837-6845.

17 M. I. Saidaminov, A. L. Abdelhady, B. Murali, E. Alarousu, V. M. Burlakov, W. Peng, I. Dursun, L. Wang, Y. He, G. Maculan, A. Goriely, T. Wu, O. F. Mohammed and O. M. Bakr, *Nat. Commun.*, 2015, **6**, 7586.

18 X. Gong, Z. Huang, R. Sabatini, C.-S. Tan, G. Bappi, G. Walters, A. Proppe, M. I. Saidaminov, O. Voznyy, S. O. Kelley and E. H. Sargent, *Nat. Commun.* 2019, **10**, 1591.

19 Y. Liu, Z. Yang, D. Cui, X. Ren, J. Sun, X. Liu, J. Zhang, Q. Wei, H. Fan, F. Yu, X. Zhang, C. Zhao and S. F. Liu, *Adv. Mater.* 2015, **27**, 5176-5183.

20 W. Wei, Y. Zhang, Q. Xu, H. Wei, Y. Fang, Q. Wang, Y. Deng, T. Li, A. Gruverman, L. Cao and J. Huang, *Nat. Photonics*, 2017, **11**, 315-321.

21 D. Liu, L. Jiang, X. Jiang, X. Sun, G. Zhang, Y.-B. Lu, Y. Wang, Z. Wu and Z. Ling, *ACS Appl. Mater. Interfaces*, 2023, **15**, 57846-57855.